IEEE Access
Multidisciplinary | Rapid Review | Open Access Journal

Received July 26, 2019, accepted August 8, 2019, date of publication August 12, 2019, date of current version August 23, 2019.

Digital Object Identifier 10.1109/ACCESS.2019.2934737

Multistatic Sonar Localization With a Transmitter

TIANYI JIA[1,2], XIAOHONG SHEN[1,2], AND HAIYAN WANG[1,3]

[1]School of Marine Science and Technology, Northwestern Polytechnical University, Xi'an 710072, China
[2]Key Laboratory of Ocean Acoustics and Sensing, Ministry of Industry and Information Technology, Northwestern Polytechnical University, Xi'an 710072, China
[3]School of Electronic Information and Artificial Intelligence, Shaanxi University of Science and Technology, Xi'an 710021, China

Corresponding author: Haiyan Wang (hywang@nwpu.edu.cn)

This work was supported in part by the National Key Research and Development Program of China under Grant 2016YFC1400200, in part by the National Natural Science Foundation of China under Grant 61571365 and Grant 61671386, and in part by the Innovation Foundation for Doctor Dissertation of Northwestern Polytechnical University under Grant CX201939.

ABSTRACT This paper focuses on the problem of multistatic sonar localization with a transmitter where the known signal transmission speed, the transmitter and receiver positions are all contaminated by Gaussian noise. The Cramér-Rao lower bound (CRLB) are derived for the object position and the localization parameters. The analysis in CRLB shows that the localization parameters have a chance to be updated to more accurate ones. Two solutions are then proposed to estimate the object position using the time measurements and angle measurements. One is a two-step closed-form solution based on weighting least squares and the other is a generalized trust region subproblem (GTRS) solution using Newton's method. A recursive MLE is also proposed to update the localization parameters and a more accurate propagation speed can be obtained from the proposed MLE especially when the propagation speed noise is large. Simulations show that the two localization solutions and the propagation speed updated from the proposed MLE can reach their CRLBs.

INDEX TERMS Multistatic sonar, active localization, CRLB, closed-form solution, GTRS, signal propagation speed.

I. INTRODUCTION

The problem of localization of an object, whether active or passive, has been an interest basis research due to its various applications in many areas, including wireless sensor networks (WSN), Internet of Thing (IoT), radar and sonar, etc [1]–[8]. As we know, most of the research focused on passive localization which are usually based on time difference of arrival (TDOA), angle of arrival (AOA), or frequency difference of arrival (FDOA), or their combinations [9]–[13]. However, when the signal emitted from the unknown object is too weak to be estimated, the performance of passive localization will deteriorate.

Active localization using multistatic sonar has robust performance and flexible applications in an underwater environment [14], [15]. When the transmitters and receivers are deployed in different positions, all the transmitters radiate acoustic signals in the same time and the passive receivers try to detect and locate the potential object from the reflected signals. The measurements used in multistatic sonar localization are similar to passive localization, including time delay, bearing angle and Doppler frequency shift, as well as their combinations. The nonlinear relationships between the object position and the measurements form a challenging estimation problem in localization.

A number of localization methods have been proposed to estimate the object position from the nonlinear measurements. The maximum likelihood estimator (MLE) [16], [17] is an accurate method which is commonly used as a benchmark in literature. However, most MLEs are time consuming by the numerical grid search technique or require good initial guess by the gradient based iterative technique. [18]–[20] proposed a type of closed-from solution which introduces nuisance variables to construct a series of linear equations and solve the equations using weighted least squares (WLS). [21] transformed the localization problem to a generalized trust region subproblem (GTRS) and solved it accurately by bisection algorithm. In [22], a three-step method based on WLS was developed to jointly estimate the position and the unknown signal propagation speed. These methods are simple and computationally efficient and they can reach the Cramér-Rao lower bound (CRLB) in the small error region. However, the parameters (sensor position or signal propagation speed) used for localization are supposed to be known exactly.

In the underwater environment, the signal propagation speed, the transmitter and receiver positions may not be known accurately [23], [24]. The errors appearing in the

The associate editor coordinating the review of this article and approving it for publication was Sajjad A. Madani.

parameters need to be taken into consideration. Hence, the mentioned methods [10]–[12], [16]–[20], [25] will not be suitable for multistatic sonar localization. The method proposed in [26], [27] took the sensor position error into account to improve the estimation accuracy and the CRLB was derived in this case.

Apart from the uncertainties of the sensor positions, the signal propagation speed or sound speed varies with depth, temperature, and salinity [23], [28], [29] in the underwater environment. This implies that the sound speed is time-variant and space-variant. Hence, there are many assumptions that have been proposed for the sound speed.

- The sound speed is a deterministic constant which is known exactly [8], [10], [20], [25]. Many localization works from the existing literature adopt this assumption.
- The sound speed is a deterministic constant which is unknown [22], [30], [31]. Because sound speed is time-variant and space-variant, it is assumed to be an unknown together with object location that could be estimated from the measurements.
- The sound speed is a random variable whose expected value and variance are known exactly [27]. The authors in [27] proposed efficient closed-form solutions for multistatic sonar localization where the sound speed is supposed to be a Gaussian random variable. A four-stage solution based on WLS was developed to estimate the object position only.
- The sound speed profile (SSP) is another commonly used model to capture the features of the propagation speed in the underwater environment [32], [33]. However, this SSP model is still complicated although it is merely a function of depth.

Considering the complexity of the underwater environment where the propagation speed together with sensor positions are all time-variant, in this paper, they are supposed to be unknown constants with respect to time during a short measurement period. During each period, the obtained localization parameters, i.e., propagation speed, the transmitter and the receiver positions are measurements of the true values and all contaminated by noise. In addition to estimating the object location, the localization parameters shall also have an opportunity to be updated to more accurate values that would work for the benefit of the applications related to these parameters. To the best of our knowledge, this scenario is not available in the existing literature.

In this paper, we focus on multistatic sonar localization with a transmitter. The localization parameters are all modeled as measurements with Gaussian noise where the true values are unknown constants. The aim of this paper is to estimate not only the object position, but also the the propagation speed. The main contributions of this work are highlighted as follows:

- The CRLBs are derived for both object position and the localization parameters. The analysis in CRLB shows that all the localization parameters have a chance to be updated to more accurate ones.
- Two solutions are proposed to estimate the object position using the time measurements and angle measurements. One is the two-step closed-form solution based on WLS and the other is the GTRS solution using Newton's method. Both solutions can reach the CRLB analytically.
- A recursive MLE based on the first order Taylor expansion of the cost function is proposed to update the localization parameters and a more accurate propagation speed can be obtained from the proposed MLE especially when the propagation speed noise is large.

The following paper will start with the measurement models in Section II. Section III derives the CRLB and gives an analysis. Section IV develops two different solutions to estimate the object position, and one solution to update the localization parameters. Section V shows the simulation results and Section VI gives the conclusion.

Notations: We use lowercase letters to represent scalars, and lowercase bold letters for column vectors, and uppercase bold letters for matrices. The symbols $\mathbf{0}$, $\mathbf{I}$ and $\mathbf{O}$ represent the zero vector, identity and zero matrices respectively, with subscript indicating their size when needed. $\mathbf{x}(i)$ is the i-th element of $\mathbf{x}$ and $\mathbf{x}(i:j)$ is a subvector formed by the i-th to the j-th element. $\|\mathbf{x}\|$ is the l_2 norm of $\mathbf{x}$. diag($\mathbf{A}$, $\mathbf{B}$) represents a block diagonal matrix whose diagonal blocks are $\mathbf{A}$ and $\mathbf{B}$. $\mathbf{A} \succeq 0$ means $\mathbf{A}$ is semi-positive definite.

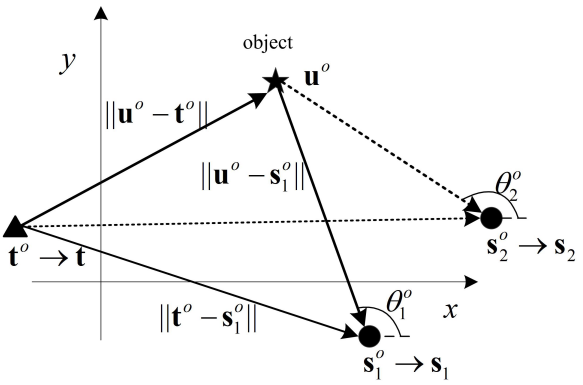

FIGURE 1. Localization scenario.

II. MEASUREMENT MODELS

We are interested in a multistatic sonar system with N receivers at $\mathbf{s}_i^o = [s_{i,x}^o, s_{i,y}^o]^T$ and a transmitter at $\mathbf{t}^o = [t_x^o, t_y^o]^T$, as shown in Fig. 1. The sonar system is used to locate an object at $\mathbf{u}^o = [x^o, y^o]^T$ by the time and bearing measurements obtained from all the receivers. The transmitter radiates a probing signal and all the receivers observe the signal through two paths: the direct propagation path from transmitter and the indirect reflection path from the object. Each receiver can obtain a differential delay time measurement of the two paths from autocorrelation technique [34] and a bearing angle measurement of the object from the array signal processing technique [35] if the conditions of these

pre-processing steps (e.g. sufficient observation period and signal bandwidth) are satisfied.

The true differential delay time τ_i^o of receiver i is

$$\tau_i^o = \frac{1}{c^o}\left(\|\mathbf{u}^o - \mathbf{t}^o\| + \|\mathbf{u}^o - \mathbf{s}_i^o\| - \|\mathbf{t}^o - \mathbf{s}_i^o\|\right). \quad (1)$$

where c^o is the signal propagation speed and $\|\cdot\|$ represents the Euclidean norm. The time measurement of receiver i is

$$\tau_i = \tau_i^o + \Delta\tau_i. \quad (2)$$

with $i = 1, 2, \cdots, N$, where $\Delta\tau_i$ is zero-mean Gaussian random noise. For notation simplicity, collecting the time measurement τ_i gives the measurement vector as

$$\boldsymbol{\tau} = \boldsymbol{\tau}^o + \Delta\boldsymbol{\tau}. \quad (3)$$

where $\boldsymbol{\tau} = [\tau_1^o, \tau_2^o, \cdots, \tau_N^o]^T$ and the noise vector $\Delta\boldsymbol{\tau} = [\Delta\tau_1, \Delta\tau_2, \cdots, \Delta\tau_N]^T$ with covariance matrix $\mathbf{Q}_\tau$.

The true bearing angle θ_i^o of receiver i depends on the object position $\mathbf{u}^o$ and the receiver position $\mathbf{s}_i^o$ by

$$\theta_i^o = \arctan\frac{y^o - s_{i,y}^o}{x^o - s_{i,x}^o}. \quad (4)$$

The angle measurement θ_i obtained by receiver i is also contaminated by zero-mean Gaussian noise,

$$\theta_i = \theta_i^o + \Delta\theta_i. \quad (5)$$

The measurement vector formed by angle measurement θ_i is

$$\boldsymbol{\theta} = \boldsymbol{\theta}^o + \Delta\boldsymbol{\theta}. \quad (6)$$

where $\boldsymbol{\theta}^o = [\theta_1^o, \theta_2^o, \cdots, \theta_N^o]^T$ and the noise vector $\Delta\boldsymbol{\theta} = [\Delta\theta_1, \Delta\theta_2, \cdots, \Delta\theta_N]^T$ with covariance matrix $\mathbf{Q}_\theta$. In this paper, the angle measurement noise and time measurement noise are supposed to be independent.

Combining the time and angle measurement together, the total measurement vector is

$$\mathbf{m} = [\boldsymbol{\tau}^T, \boldsymbol{\theta}^T]^T = \mathbf{m}^o + \Delta\mathbf{m} \quad (7)$$

where $\Delta\mathbf{m} = [\Delta\boldsymbol{\tau}^T, \Delta\boldsymbol{\theta}^T]^T$ is the measurement noise vector with covariance matrix $\mathbf{Q}_m = \mathrm{diag}(\mathbf{Q}_\tau, \mathbf{Q}_\theta)$.

In the underwater environment for sonar localization, the parameters including transmitter position $\mathbf{t}^o$, receiver position $\mathbf{s}_i^o$ and signal propagation speed c^o are not accurately known to an estimator. In fact, only the nominal parameter values $\mathbf{t}$, $\mathbf{s}_i$ and c are available for the estimator, rather than their true values. In this paper, the nominal parameters are measurements of the true values and they are supposed to be

$$c = c^o + \Delta c \quad (8a)$$

$$\mathbf{t} = \mathbf{t}^o + \Delta\mathbf{t} \quad (8b)$$

$$\mathbf{s}_i = \mathbf{s}_i^o + \Delta\mathbf{s}_i \quad (8c)$$

where Δc, $\Delta\mathbf{t}$ and $\Delta\mathbf{s}_i$ are also zero-mean Gaussian noise. The noises of all parameters and the noises of all measurements are supposed to be independent with each other. The variance of Δc is σ_c^2. For notation simplicity, we collect the transmitter and receiver positions as $\mathbf{p} = [\mathbf{t}^T, \mathbf{s}_1^T, \mathbf{s}_2^T, \cdots, \mathbf{s}_N^T]^T$, and the corresponding sensor position noise is $\Delta\mathbf{p}$ with covariance matrix $\mathbf{Q}_p$. In the following, the general term sensor will be used to represent transmitter and receiver.

We would like to estimate the object position $\mathbf{u}^o$ from the time and angle measurements $\mathbf{m}$ together with the inaccurate transmission speed c and sensor position $\mathbf{p}$. In addition, transmission speed c or sensor position $\mathbf{p}$ will also be updated because the analysis shows that the nominal values of all parameters have a chance to be updated to more accurate ones.

III. CRLB AND ANALYSIS

A. CRLB

We are interested in evaluating the CRLB of the multistatic sonar localization when considering the effect of signal propagation speed error and the sensor position errors. Define the unknown vector as $\boldsymbol{\alpha}^o = [\mathbf{u}^{oT}, c^o, \mathbf{p}^{oT}]^T$, the measurement vector $\mathbf{m}$, the transmission speed c and sensor position $\mathbf{p}$ are Gaussian distributed, and these measurements are independent with each other. Therefore, the joint probability distribution function for $\mathbf{m}$, c and $\mathbf{p}$ is

$$f(\mathbf{m}, c, \mathbf{p}) = f_1(\mathbf{m}|c, \mathbf{p})f_2(c)f_3(\mathbf{p}), \quad (9)$$

where $f_1(\mathbf{m}|c, \mathbf{p})$ is the conditional probability distribution function of $\mathbf{m}$ given c and $\mathbf{p}$. $f_2(c)$ and $f_3(\mathbf{p})$ are the distribution functions of c and $\mathbf{p}$ respectively. Taking logarithm of (9) and rearranging yield

$$\begin{aligned}\ln f(\mathbf{m}, c, \mathbf{p}) &= \ln f_1(\mathbf{m}|c, \mathbf{p}) + \ln f_2(c) + \ln f_3(\mathbf{p}) \\ &= k - \frac{1}{2}(\mathbf{m}-\mathbf{m}^o)^T\mathbf{Q}_m^{-1}(\mathbf{m}-\mathbf{m}^o) \\ &\quad - \frac{(c-c^o)^2}{2\sigma_c^2} - \frac{1}{2}(\mathbf{p}-\mathbf{p}^o)^T\mathbf{Q}_p^{-1}(\mathbf{p}-\mathbf{p}^o) \end{aligned} \quad (10)$$

where k is a constant which is independent of $\boldsymbol{\alpha}^o$.

The CRLB of $\boldsymbol{\alpha}^o$ is given by

$$\mathrm{CRLB}(\boldsymbol{\alpha}^o) = \mathrm{FIM}(\boldsymbol{\alpha}^o)^{-1} \quad (11)$$

where $\mathrm{FIM}(\boldsymbol{\alpha}^o)$ is the Fisher information matrix. It can be expressed as [36]

$$\mathrm{FIM}(\boldsymbol{\alpha}^o) = E\left[\frac{\partial \ln f(\mathbf{m}, c, \mathbf{p})}{\partial\boldsymbol{\alpha}^o}\frac{\partial \ln f(\mathbf{m}, c, \mathbf{p})}{\partial\boldsymbol{\alpha}^{oT}}\right] \quad (12)$$

where

$$\frac{\partial \ln f(\mathbf{m}, c, \mathbf{p})}{\partial\boldsymbol{\alpha}^{oT}} = \frac{\partial \ln f_1(\mathbf{m}|c, \mathbf{p})}{\partial\boldsymbol{\alpha}^{oT}} + \frac{\partial \ln f_2(c)}{\partial\boldsymbol{\alpha}^{oT}} + \frac{\partial \ln f_3(\mathbf{p})}{\partial\boldsymbol{\alpha}^{oT}} \quad (13)$$

and

$$\frac{\partial \ln f_1(\mathbf{m}|c, \mathbf{p})}{\partial\boldsymbol{\alpha}^{oT}} = (\mathbf{m} - \mathbf{m}^o)^T\mathbf{Q}_m^{-1}\frac{\partial\mathbf{m}^o}{\partial\boldsymbol{\alpha}^{oT}} \quad (14a)$$

$$\frac{\partial \ln f_2(c)}{\partial\boldsymbol{\alpha}^{oT}} = [\mathbf{0}_2^T, (c-c^o)\sigma_c^{-2}, \mathbf{0}_{2N+2}^T] \quad (14b)$$

$$\frac{\partial \ln f_3(\mathbf{p})}{\partial\boldsymbol{\alpha}^{oT}} = [\mathbf{0}_2^T, 0, (\mathbf{p} - \mathbf{p}^o)^T\mathbf{Q}_p^{-1}]. \quad (14c)$$

The notation $E[\cdot]$ represents the expectation and $\partial \mathbf{m}^o / \partial \boldsymbol{\alpha}^{oT}$ is in Appendix A. After putting (13) and (14) in (12), the expectation can be expressed as [26]

$$\mathrm{FIM}(\boldsymbol{\alpha}^o) = \begin{bmatrix} \mathbf{X} & \mathbf{Y} \\ \mathbf{Y}^T & \mathbf{Z} + \boldsymbol{\Lambda} \end{bmatrix} \tag{15}$$

where

$$\begin{aligned} \mathbf{X} &= \frac{\partial \mathbf{m}^{oT}}{\partial \mathbf{u}^o} \mathbf{Q}_m^{-1} \frac{\partial \mathbf{m}^o}{\partial \mathbf{u}^{oT}} \\ \mathbf{Y} &= \frac{\partial \mathbf{m}^{oT}}{\partial \mathbf{u}^o} \mathbf{Q}_m^{-1} \frac{\partial \mathbf{m}^o}{\partial \boldsymbol{\varrho}^{oT}} \\ \mathbf{Z} &= \frac{\partial \mathbf{m}^{oT}}{\partial \boldsymbol{\varrho}^o} \mathbf{Q}_m^{-1} \frac{\partial \mathbf{m}^o}{\partial \boldsymbol{\varrho}^{oT}} \\ \boldsymbol{\Lambda} &= \mathrm{diag}(\sigma_c^{-2}, \mathbf{Q}_p^{-1}) \end{aligned} \tag{16}$$

and $\boldsymbol{\varrho}^o = [c^o, \mathbf{p}^{oT}]^T$ is the true value vector of the localization parameters. The upper left block 2×2 of (11) gives the CRLB of object location. Substituting (15) in (11) and using the partitioned matrix inversion formula yield

$$\mathrm{CRLB}(\mathbf{u}^o) = \left(\mathbf{X} - \mathbf{Y}(\mathbf{Z} + \boldsymbol{\Lambda})^{-1} \mathbf{Y}^T \right)^{-1}. \tag{17}$$

The CRLB for c^o and $\mathbf{p}^o$ can also be obtained as

$$\mathrm{CRLB}(\boldsymbol{\varrho}^o) = \left(\mathbf{Z} + \boldsymbol{\Lambda} - \mathbf{Y}^T \mathbf{X}^{-1} \mathbf{Y} \right)^{-1}. \tag{18}$$

B. ANALYSIS

1) THE NOMINAL PARAMETER NOISE IS INSIGNIFICANT

When the noises of nominal parameters, i.e., Δc and $\Delta \mathbf{p}$ are relatively small compared with the measurement noise $\Delta \mathbf{m}$, we can approximate $\left(\mathbf{Z} + \boldsymbol{\Lambda} - \mathbf{Y}^T \mathbf{X}^{-1} \mathbf{Y} \right)^{-1}$ as $\boldsymbol{\Lambda}^{-1}$. Hence, the CRLB of $\boldsymbol{\varrho}^o$ can be approximated as

$$\mathrm{CRLB}(\boldsymbol{\varrho}^o) \approx \boldsymbol{\Lambda}^{-1} = \mathrm{diag}(\sigma_c^2, \mathbf{Q}_p) \tag{19}$$

where $\boldsymbol{\Lambda}^{-1}$ is the covariance matrix of the nominal parameter vector $\boldsymbol{\varrho}$.

2) THE NOMINAL PARAMETER NOISE IS SIGNIFICANT

When the nominal parameter noise is significant, (19) will not be accurate. Invoking the Woodbury identity in (19) that

$$\mathrm{CRLB}(\boldsymbol{\varrho}^o) = \boldsymbol{\Lambda}^{-1} - \left(\boldsymbol{\Lambda}(\mathbf{Z} - \mathbf{Y}^T \mathbf{X}^{-1} \mathbf{Y})^{-1} \boldsymbol{\Lambda} + \boldsymbol{\Lambda} \right)^{-1}. \tag{20}$$

Note that $(\mathbf{Z} - \mathbf{Y}^T \mathbf{X}^{-1} \mathbf{Y})^{-1}$ represents the CRLB of $\boldsymbol{\varrho}^o$ when the nominal values of c^o and $\mathbf{p}^o$ are not available. We also know that $\boldsymbol{\Lambda}^{-1}$ is the covariance matrix of the nominal parameter vector $\boldsymbol{\varrho}$ before estimation, and $\mathrm{CRLB}(\boldsymbol{\varrho}^o)$ is the lower bound of the covariance matrix after estimation. Obviously the second term in (20) is a definite matrix by applying the properties of definite matrix. Therefore

$$\boldsymbol{\Lambda}^{-1} \succeq \mathrm{CRLB}(\boldsymbol{\varrho}^o) \tag{21}$$

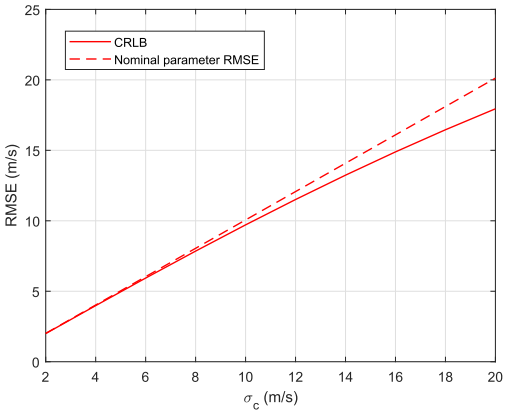

FIGURE 2. Comparison of the CRLB and the nominal parameter RMSE for the signal propagation speed c^o.

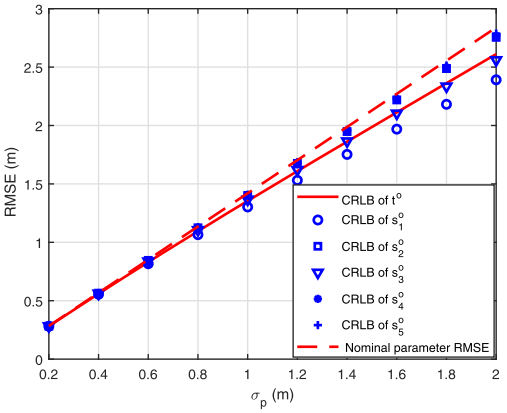

FIGURE 3. Comparisons of the CRLBs and the nominal parameter RMSE for the sensor (transmitter t^o and receiver s_l^o) position.

which means the nominal values of c and $\mathbf{p}$ shall be updated to more accurate ones through the time and angle measurements.

Fig. 2 and Fig. 3 show an example of the CRLB for the nominal parameter. The setting is the same as in Section V, where $\mathbf{Q}_\tau = (\sigma/c^o)^2 \mathbf{I}$, $\mathbf{Q}_\theta = \sigma_\theta^2 \mathbf{I}$ and $\mathbf{Q}_p = \sigma_p^2 \mathbf{I}$. In the figures, $\sigma = 1$ m and $\sigma_\theta = 1$ deg. We set $\sigma_p = 1$ m in Fig. 2 and $\sigma_c = 5$ m/s in Fig. 3 respectively. Fig. 2 shows that the CRLB of signal propagation speed c^o is lower than the nominal parameter RMSE all the time and the the gap between them will become significant when the noise variance of c^o increases. When σ_c is small, the CRLB is closed to the nominal parameter RMSE. Fig. 3 gives the CRLBs for all sensor positions and the nominal parameter RMSEs for them. Because their nominal parameter RMSEs are the same, the figure only shows one nominal parameter RMSE. As expected from the analysis, all the position CRLBs are lower than the RMSEs. However, the gaps among the CRLBs and the nominal parameter RMSE are not significant for all sensors even though the position noise σ_p is large. In addition, the extensive Monte Carlo simulation tests in Section V also show that it is not possible to update all the sensor positions using the proposed method so that they can reach their CRLBs.

IV. LOCALIZATION SOLUTION AND PARAMETER UPDATE

In this section, two different solutions will be proposed to estimate the location of object. One is the algebraic closed-form solution that advances the previous research [27] and reduces the computational complexity by decreasing the solution steps from 4 to 2. The other is the GTRS solution using Newton's method that has faster convergence speed compared with the GTRS solution based on the bisection algorithm [21]. In addition to the object location, the solution based on maximum likelihood estimation (MLE) will also be proposed to update the localization parameters to more accurate values, which is very different from the existing work, and this is also another major contribution of our work.

A. 2-STEP CLOSED-FORM SOLUTION

1) FIRST STEP

We will transform the measurement equations (1) and (4) to linear equations using the available nominal values of parameters. The items in (1) can be Taylor expanded as

$$\|\mathbf{u}^o - \mathbf{t}^o\| \approx \|\mathbf{u}^o - \mathbf{t}\| + \boldsymbol{\rho}_{\mathbf{u}^o-\mathbf{t}}^T \Delta\mathbf{t} \tag{22a}$$

$$\|\mathbf{u}^o - \mathbf{s}_i^o\| \approx \|\mathbf{u}^o - \mathbf{s}_i\| + \boldsymbol{\rho}_{\mathbf{u}^o-\mathbf{s}_i}^T \Delta\mathbf{s}_i \tag{22b}$$

$$\|\mathbf{t}^o - \mathbf{s}_i^o\| \approx \|\mathbf{t} - \mathbf{s}_i\| + \boldsymbol{\rho}_{\mathbf{t}-\mathbf{s}_i}^T (\Delta\mathbf{s}_i - \Delta\mathbf{t}) \tag{22c}$$

where $\boldsymbol{\rho}_{\mathbf{a}} = \mathbf{a}/\|\mathbf{a}\|$ defines the unit length vector of $\mathbf{a}$. Substituting (2), (8a) and (22) in (1) and neglecting the second-order noise terms yield

$$c\tau_i \approx \|\mathbf{u}^o - \mathbf{t}\| + \|\mathbf{u}^o - \mathbf{s}_i\| - \|\mathbf{t} - \mathbf{s}_i\| + n_{\tau,i} \tag{23}$$

where

$$n_{\tau,i} = \tau_i \Delta c + c\Delta\tau_i + \boldsymbol{\rho}_{\mathbf{u}^o-\mathbf{t}}^T \Delta\mathbf{t} + \boldsymbol{\rho}_{\mathbf{u}^o-\mathbf{s}_i}^T \Delta\mathbf{s}_i - \boldsymbol{\rho}_{\mathbf{t}-\mathbf{s}_i}^T (\Delta\mathbf{s}_i - \Delta\mathbf{t}). \tag{24}$$

Moving the item $\|\mathbf{u}^o-\mathbf{t}\|-\|\mathbf{t}-\mathbf{s}_i\|$ from right to left, squaring both sides and rearranging form

$$2\|\mathbf{u}^o - \mathbf{s}_i\| n_{\tau,i} = c^2\tau_i^2 + 2c\tau_i\|\mathbf{t} - \mathbf{s}_i\| + 2\mathbf{t}^T(\mathbf{t}-\mathbf{s}_i) - 2(\mathbf{t}-\mathbf{s}_i)^T\mathbf{u}^o - 2(c\tau_i + \|\mathbf{t} - \mathbf{s}_i\|)\|\mathbf{u}^o - \mathbf{t}\| \tag{25}$$

where the second-order noise term is ignored. Let $\boldsymbol{\varphi}^o = [\mathbf{u}^{oT}, \|\mathbf{u}^o - \mathbf{t}\|]^T$, and (25) can be transformed to a linear equation in matrix form

$$\mathbf{B}_\tau \mathbf{n}_\tau = \mathbf{h}_\tau - \mathbf{G}_\tau \boldsymbol{\varphi}^o \tag{26}$$

where $\mathbf{n}_\tau = \boldsymbol{\tau}\Delta c + c\Delta\boldsymbol{\tau} + \mathbf{D}_1\Delta\mathbf{p}$. The related matrices are

$$\mathbf{B}_\tau = \begin{bmatrix} 2\|\mathbf{u}^o - \mathbf{s}_1\| & \cdots & 0 \\ \vdots & \ddots & \vdots \\ 0 & \cdots & 2\|\mathbf{u}^o - \mathbf{s}_N\| \end{bmatrix} \tag{27a}$$

$$\mathbf{h}_\tau = \begin{bmatrix} c^2\tau_1^2 + 2c\tau_1\|\mathbf{t} - \mathbf{s}_1\| + 2\mathbf{t}^T(\mathbf{t} - \mathbf{s}_1) \\ \vdots \\ c^2\tau_N^2 + 2c\tau_i\|\mathbf{t} - \mathbf{s}_N\| + 2\mathbf{t}^T(\mathbf{t} - \mathbf{s}_N) \end{bmatrix} \tag{27b}$$

$$\mathbf{G}_\tau = \begin{bmatrix} 2(\mathbf{t} - \mathbf{s}_1)^T & 2(c\tau_1 + \|\mathbf{t} - \mathbf{s}_1\|) \\ \vdots & \vdots \\ 2(\mathbf{t} - \mathbf{s}_N)^T & 2(c\tau_N + \|\mathbf{t} - \mathbf{s}_N\|) \end{bmatrix} \tag{27c}$$

$$\mathbf{D}_1 = \begin{bmatrix} \vdots & \ddots & \\ \boldsymbol{\rho}_{\mathbf{u}^o-\mathbf{t}}^T + \boldsymbol{\rho}_{\mathbf{t}-\mathbf{s}_i}^T & \boldsymbol{\rho}_{\mathbf{u}^o-\mathbf{s}_i}^T - \boldsymbol{\rho}_{\mathbf{t}-\mathbf{s}_i}^T & \\ \vdots & & \ddots \end{bmatrix}. \tag{27d}$$

Next we will construct a linear equation related to angle from (4). Define $\boldsymbol{\nu}_i^o = [-\sin\theta_i^o, \cos\theta_i^o]^T$, (4) can be expressed as

$$\boldsymbol{\nu}_i^{oT}(\mathbf{u}^o - \mathbf{s}_i^o) = 0. \tag{28}$$

The Taylor expansion of $\boldsymbol{\nu}_i^o$ is

$$\boldsymbol{\nu}_i^o = \boldsymbol{\nu}_i + \dot{\boldsymbol{\nu}}_i \Delta\theta_i \tag{29}$$

where $\boldsymbol{\nu}_i = [-\sin\theta_i, \cos\theta_i]^T$ and $\dot{\boldsymbol{\nu}}_i = [\cos\theta_i, \sin\theta_i]^T$. Substituting (8c) and (29), ignoring the second-order noise term, (28) becomes

$$\boldsymbol{\nu}_i^T\Delta\mathbf{s}_i + \dot{\boldsymbol{\nu}}_i^T(\mathbf{u}^o - \mathbf{s}_i)\Delta\theta_i = \boldsymbol{\nu}_i^T\mathbf{s}_i - \boldsymbol{\nu}_i^T\mathbf{u}^o. \tag{30}$$

This is a linear equation of $\mathbf{u}^o$ and the matrix form is

$$\mathbf{n}_\theta = \mathbf{h}_\theta - \mathbf{G}_\theta\mathbf{u}^o \tag{31}$$

where $\mathbf{n}_\theta = \mathbf{B}_\theta\Delta\boldsymbol{\theta} + \mathbf{D}_2\Delta\mathbf{p}$ and the related matrices are

$$\mathbf{B}_\theta = \begin{bmatrix} \dot{\boldsymbol{\nu}}_1^T(\mathbf{u}^o - \mathbf{s}_1) & \cdots & 0 \\ \vdots & \ddots & \vdots \\ 0 & \cdots & \dot{\boldsymbol{\nu}}_N^T(\mathbf{u}^o - \mathbf{s}_N) \end{bmatrix}, \tag{32}$$

$$\mathbf{D}_2 = \begin{bmatrix} 0 & \boldsymbol{\nu}_1^T & \cdots & 0 \\ \vdots & \vdots & \ddots & \vdots \\ 0 & 0 & \cdots & \boldsymbol{\nu}_N^T \end{bmatrix}, \tag{33}$$

$$\mathbf{h}_\theta = \begin{bmatrix} \boldsymbol{\nu}_1^T\mathbf{s}_1 \\ \vdots \\ \boldsymbol{\nu}_N^T\mathbf{s}_N \end{bmatrix} \quad \mathbf{G}_\theta = \begin{bmatrix} \boldsymbol{\nu}_1^T \\ \vdots \\ \boldsymbol{\nu}_N^T \end{bmatrix}. \tag{34}$$

Stacking (26) and (31) together yields the solution equation using both time and bearing measurements in the first step as

$$\mathbf{n} = \mathbf{h}_1 - \mathbf{G}_1\boldsymbol{\varphi}^o \tag{35}$$

where

$$\mathbf{n} = \begin{bmatrix} \mathbf{B}_\tau\mathbf{n}_\tau \\ \mathbf{n}_\theta \end{bmatrix}, \quad \mathbf{h}_1 = \begin{bmatrix} \mathbf{h}_\tau \\ \mathbf{h}_\theta \end{bmatrix}, \quad \mathbf{G}_1 = \begin{bmatrix} \mathbf{G}_\tau & \\ \mathbf{G}_\theta & \mathbf{0}_N \end{bmatrix}. \tag{36}$$

Finally the closed-form solution using weighted least squares (WLS) method in the first step is

$$\boldsymbol{\varphi} = (\mathbf{G}_1^T\mathbf{W}_1\mathbf{G}_1)^{-1}\mathbf{G}_1^T\mathbf{W}_1\mathbf{h}_1 \tag{37}$$

where the weighting matrix $\mathbf{W}_1 = (E[\mathbf{n}\mathbf{n}^T])^{-1} \equiv \mathbf{Q}_n^{-1}$ is given in

$$\mathbf{Q}_n = \begin{bmatrix} \mathbf{B}_\tau \mathbf{Q}_{n,\tau} \mathbf{B}_\tau^T & \mathbf{B}_\tau \mathbf{D}_1 \mathbf{Q}_p \mathbf{D}_2^T \\ \mathbf{D}_2 \mathbf{Q}_p \mathbf{D}_1^T \mathbf{B}_\tau^T & \mathbf{B}_\theta \mathbf{Q}_\theta \mathbf{B}_\theta^T + \mathbf{D}_2 \mathbf{Q}_p \mathbf{D}_2^T \end{bmatrix} \tag{38}$$

and

$$\mathbf{Q}_{n,\tau} \equiv (E[\mathbf{n}_\tau \mathbf{n}_\tau^T]) = \sigma_c^2 \boldsymbol{\tau}\boldsymbol{\tau}^T + c^2 \mathbf{Q}_\tau + \mathbf{D}_1 \mathbf{Q}_p \mathbf{D}_1^T. \tag{39}$$

Note that $\mathbf{W}_1$ needs the true value of objection position $\mathbf{u}^o$. We can first set the nonzero element related to $\mathbf{u}^o$ in $\mathbf{W}_1$ as 1 to obtain an initial location estimate, and then $\mathbf{W}_1$ in the first step shall be estimated using the initial location. When the noise is not large, it can be shown that

$$E[\boldsymbol{\varphi}] \approx (\mathbf{G}_1^T \mathbf{W}_1 \mathbf{G}_1)^{-1} \mathbf{G}_1^T \mathbf{W}_1 (\mathbf{G}_1 \boldsymbol{\varphi}^o) = \boldsymbol{\varphi}^o, \tag{40a}$$

$$\mathrm{cov}(\boldsymbol{\varphi}) = E[\boldsymbol{\varphi}\boldsymbol{\varphi}^T] - E[\boldsymbol{\varphi}]E[\boldsymbol{\varphi}^T] \approx (\mathbf{G}_1^T \mathbf{W}_1 \mathbf{G}_1)^{-1}. \tag{40b}$$

However, the solution in first step cannot reach the CRLB because the relation between $\mathbf{u}^o$ and $\|\mathbf{u}^o - \mathbf{t}\|$ is not considered. Next step the solution $\boldsymbol{\varphi}$ will be updated to a more accurate solution.

2) SECOND STEP

This step exploits the relationship to improve accuracy. Suppose $\boldsymbol{\varphi} = \boldsymbol{\varphi}^o + \Delta\boldsymbol{\varphi}$, the relationship between $\boldsymbol{\varphi}(1:2)$ and $\boldsymbol{\varphi}(3)$ is

$$\begin{aligned}(\boldsymbol{\varphi}(3) - \Delta\boldsymbol{\varphi}(3))^2 &= \boldsymbol{\varphi}^o(3)^2 = (\|\mathbf{u}^o - \mathbf{t}\|)^2 \\ &= \|\boldsymbol{\varphi}(1:2) - \Delta\boldsymbol{\varphi}(1:2)\|^2 + \|\mathbf{t}\|^2 - 2\mathbf{t}^T\mathbf{u}^o.\end{aligned} \tag{41}$$

We also have an additional equation

$$\Delta\boldsymbol{\varphi}(1:2) = \boldsymbol{\varphi}(1:2) - \mathbf{u}^o. \tag{42}$$

Ignoring the second order noise terms in (41) and combining with (42), we have

$$\mathbf{B}_2 \Delta\boldsymbol{\varphi} \approx \mathbf{h}_2 - \mathbf{G}_2 \mathbf{u}^o \tag{43}$$

where

$$\mathbf{B}_2 = \begin{bmatrix} \mathbf{I}_2 & \mathbf{0}_2 \\ 2\boldsymbol{\varphi}^T(1:2) & -2\boldsymbol{\varphi}(3) \end{bmatrix}, \quad \mathbf{G}_2 = \begin{bmatrix} \mathbf{I}_2 \\ 2\mathbf{t}^T \end{bmatrix}, \tag{44a}$$

$$\mathbf{h}_2 = \begin{bmatrix} \boldsymbol{\varphi}_1(1:2) \\ \|\boldsymbol{\varphi}_1(1:2)\|^2 - \boldsymbol{\varphi}(3)^2 + \|\mathbf{t}\|^2 \end{bmatrix}. \tag{44b}$$

The WLS solution to (43) is

$$\mathbf{u} = (\mathbf{G}_2^T \mathbf{W}_2 \mathbf{G}_2)^{-1} \mathbf{G}_2^T \mathbf{W}_2 \mathbf{h}_2 \tag{45}$$

where the weighting matrix $\mathbf{W}_2 = (\mathbf{B}_2 \mathrm{cov}(\boldsymbol{\varphi}) \mathbf{B}_2^T)^{-1}$. When the noise is small, it can be shown that

$$\mathrm{cov}(\mathbf{u}) \approx (\mathbf{G}_2^T \mathbf{W}_2 \mathbf{G}_2)^{-1}. \tag{46}$$

After substituting the expressions of $\mathbf{W}_2$, $\mathrm{cov}(\boldsymbol{\varphi})$ and $\mathbf{W}_1$ in (46) one after another, $\mathrm{cov}(\mathbf{u})$ becomes

$$\mathrm{cov}(\mathbf{u})^{-1} = \mathbf{G}_2^T \mathbf{B}_2^{-T} \mathbf{G}_1^T \mathbf{Q}_n^{-1} \mathbf{G}_1 \mathbf{B}_2^{-1} \mathbf{G}_2 \tag{47}$$

where $\mathbf{Q}_n$ is in (38). Putting (39) in (38) and rearranging produce

$$\mathbf{Q}_n = \mathbf{B}_1 \left(\mathbf{Q}_m + \mathbf{D}_3 \boldsymbol{\Lambda}^{-1} \mathbf{D}_3^T \right) \mathbf{B}_1^T \tag{48}$$

where $\mathbf{Q}_m$ is defined under (7) and $\boldsymbol{\Lambda}$ is in (16), and

$$\mathbf{B}_1 = \begin{bmatrix} c\mathbf{B}_\tau & \mathbf{O} \\ \mathbf{O} & \mathbf{B}_\theta \end{bmatrix}, \quad \mathbf{D}_3 = \begin{bmatrix} \boldsymbol{\tau}/c & \mathbf{D}_1/c \\ \mathbf{0} & \mathbf{B}_\theta^{-1}\mathbf{D}_2 \end{bmatrix}. \tag{49}$$

Substituting (48) in (47) and invoking Woodbury matrix identity shall give the final expression of $\mathrm{cov}(\mathbf{u})^{-1}$ as

$$\begin{aligned}\mathrm{cov}(\mathbf{u})^{-1} &= \mathbf{D}_4 \mathbf{Q}_m^{-1} \mathbf{D}_4^T \\ &\quad - \mathbf{D}_4 \mathbf{Q}_m^{-1} \mathbf{D}_3 \left(\mathbf{D}_3 \mathbf{Q}_m^{-1} \mathbf{D}_3^T + \boldsymbol{\Lambda} \right)^{-1} \mathbf{D}_3^T \mathbf{Q}_m^{-1} \mathbf{D}_4^T\end{aligned} \tag{50}$$

where $\mathbf{D}_4 = \mathbf{G}_2^T \mathbf{B}_2^{-T} \mathbf{G}_1^T \mathbf{B}_1^{-T}$. On the other hand, the inverse of the CRLB in (17) is

$$\mathrm{CRLB}(\mathbf{u}^o)^{-1} = \mathbf{X} - \mathbf{Y}(\mathbf{Z} + \boldsymbol{\Lambda})^{-1} \mathbf{Y}^T \tag{51}$$

where $\mathbf{X}$, $\mathbf{Y}$ and $\mathbf{Z}$ is shown in (16). Comparing (50) and (51) implies that $\mathrm{cov}(\mathbf{u})$ and $\mathrm{CRLB}(\mathbf{u}^o)$ have the same form of expression. If the noise is small enough so that the effect in the related matrices is insignificant, it can be verified through some algebraic manipulations that

$$\mathbf{D}_3 \approx -\frac{\partial \mathbf{m}^o}{\partial \boldsymbol{\varrho}^{oT}}, \quad \mathbf{D}_4 \approx \frac{\partial \mathbf{m}^{oT}}{\partial \mathbf{u}^o}. \tag{52}$$

Therefore under small noise assumption, we conclude from (50)–(52) and (16) that

$$\mathrm{cov}(\mathbf{u}) \approx \mathrm{CRLB}(\mathbf{u}^o). \tag{53}$$

Remark 1: The 2-step closed-form solution proposed in this section can be simplified to the other closed-form solution when we ignore the nominal parameter error. The processing step follows the same procedure except for the weighting matrix in (37) replaced by the modified weighting matrix $\tilde{\mathbf{W}}_1 = \tilde{\mathbf{Q}}_n^{-1}$ and

$$\tilde{\mathbf{Q}}_n = \begin{bmatrix} c^2 \mathbf{B}_\tau \mathbf{Q}_\tau \mathbf{B}_\tau^T & \mathbf{O} \\ \mathbf{O} & \mathbf{B}_\theta \mathbf{Q}_\theta \mathbf{B}_\theta^T \end{bmatrix}. \tag{54}$$

When the measurement noise is larger than the parameter noise, the weighting matrix will be dominated by $\mathbf{Q}_m$ and $\mathbf{Q}_n \approx \tilde{\mathbf{Q}}_n$. Hence, these two solutions will have the similar performance.

B. GTRS SOLUTION

The localization problem (35) can be transformed to a constrained weighted least squares (CWLS) problem

$$\min_{\boldsymbol{\varphi}^o \in \mathbb{R}^3} (\mathbf{h}_1 - \mathbf{G}_1 \boldsymbol{\varphi}^o)^T \mathbf{W}_1 (\mathbf{h}_1 - \mathbf{G}_1 \boldsymbol{\varphi}^o) \tag{55a}$$

$$\text{s.t. } (\boldsymbol{\varphi}^o - \boldsymbol{a})^T \boldsymbol{\Sigma} (\boldsymbol{\varphi}^o - \boldsymbol{a}) = 0 \tag{55b}$$

where $\boldsymbol{\Sigma} = \mathrm{diag}([1, 1, -1])$, and $\boldsymbol{a} = [\mathbf{t}^T, 0]^T$. Note that (55) is a minimization of a quadratic function subject to a

single quadratic constraint. Problems of this type are called generalized trust region subproblems (GTRS) [21], [37].

Defining a Lagrange multiplier λ, the augmented cost function is

$$J(\boldsymbol{\varphi}^o, \lambda) = (\mathbf{h}_1 - \mathbf{G}_1\boldsymbol{\varphi}^o)^T\mathbf{W}_1(\mathbf{h}_1 - \mathbf{G}_1\boldsymbol{\varphi}^o) + \lambda(\boldsymbol{\varphi}^o - \boldsymbol{a})^T\boldsymbol{\Sigma}(\boldsymbol{\varphi}^o - \boldsymbol{a}). \quad (56)$$

Taking the partial derivative of $J(\boldsymbol{\varphi}^o, \lambda)$ with respect to $\boldsymbol{\varphi}^o$ and setting the term to zeros produce

$$\boldsymbol{\varphi}(\lambda) = (\mathbf{G}_1^T\mathbf{W}_1\mathbf{G}_1 + \lambda\boldsymbol{\Sigma})^{-1}(\mathbf{G}_1^T\mathbf{W}_1\mathbf{h}_1 + \lambda\boldsymbol{\Sigma}\boldsymbol{a}). \quad (57)$$

Substituting (57) into the constraint (55b), a nonlinear equation related to λ is obtained as

$$f(\lambda) \triangleq (\boldsymbol{\varphi}(\lambda) - \boldsymbol{a})^T\boldsymbol{\Sigma}(\boldsymbol{\varphi}(\lambda) - \boldsymbol{a}). \quad (58)$$

We can gain some insight from (56)-(58). When the measurement $\mathbf{m}$ and these nominal parameters (c, $\mathbf{t}$ and $\mathbf{s}_i$) in (56) are all replaced by the true values ($\mathbf{m}^o$, c^o, $\mathbf{t}^o$ and $\mathbf{s}_i^o$), the augmented cost function shall have a minimum value equal to 0 and the optimal λ is equal to 0 which is also a root of $f(\lambda)$. This means when the noise appearing in the estimator is not large, the optimal λ is the root of $f(\lambda)$ which is close to 0. That is to say, $f(\lambda)$ has a root which is close to 0 and this root is the optimal λ. Therefore a simple Newton's method can be used to search for the root of $f(\lambda)$. The solution for GTRS using Newton's method is summarized in the following algorithm.

Algorithm 1 GTRS Solution Using Newton's Method

Input: The constructed parameters $\mathbf{h}_1$, $\mathbf{G}_1$, $\mathbf{W}_1$, $\boldsymbol{\Sigma}$, $\boldsymbol{a}$ and the initial guess $\lambda^0 = \Delta\lambda$ and $\lambda^1 = 0$

Output: An estimate $\boldsymbol{\varphi}$ and λ

```
while k is less than a given number of iterations do
    Compute f(λ^k) using (58)
    if f(λ^k) − f(λ^{k−1}) is less than a given threshold level then
        Compute φ(λ^k) using (57)
        return φ(λ^k) and λ^k
    else
        Update λ using λ^{k+1} = (λ^{k−1} f(λ^k) − λ^k f(λ^{k−1})) / (f(λ^k) − f(λ^{k−1}))
        k = k + 1
return result
```

This algorithm also needs an initial estimate for $\mathbf{W}_1$ and it is described below (39). The initial value $\Delta\lambda$ is a small value which is used to approximate the derivative of $f(\lambda)$ with respect to λ when $\lambda = 0$.

The performance analysis of GTRS is to recast the CWLS problem in (55) to a unconstrained minimization problem, and then formulate the relationship between them. First, consider the following unconstrained minimization problem by removing the constrain in (55)

$$\boldsymbol{\varphi} = \arg\min_{\boldsymbol{\varphi}^o \in \mathbb{R}^3}(\mathbf{h}_1 - \mathbf{G}_1\boldsymbol{\varphi}^o)^T\mathbf{W}_1(\mathbf{h}_1 - \mathbf{G}_1\boldsymbol{\varphi}^o). \quad (59)$$

This is a unconstrained WLS problem of $\boldsymbol{\varphi}^o$, and the solution and its covariance matrix are shown in (37) and (40b) respectively. The imposing constrain (55b) formulates a projection between $\boldsymbol{\varphi}^o$ and $\mathbf{u}^o$ that can be expressed as

$$\boldsymbol{\varphi}^o(\mathbf{u}^o) = [\mathbf{u}^{oT}, \|\mathbf{u}^o - \mathbf{t}\|]^T \quad (60)$$

where $\boldsymbol{\varphi}^o(\mathbf{u}^o)$ is parametric form of $\boldsymbol{\varphi}^o$ in terms of $\mathbf{u}^o$. By defining the covariance matrices of (55) and (59) as $\mathrm{cov}_{\mathrm{con}}$ and $\mathrm{cov}_{\mathrm{un}}$, the relationship between them is

$$\mathrm{cov}_{\mathrm{un}} = \mathbf{F}\,\mathrm{cov}_{\mathrm{con}}\,\mathbf{F}^T \quad (61)$$

where

$$\mathbf{F} = \frac{\partial\boldsymbol{\varphi}^o(\mathbf{u}^o)}{\partial\mathbf{u}^{oT}} = \begin{bmatrix}\mathbf{I}_2 \\ \boldsymbol{\rho}_{\mathbf{u}^o-\mathbf{t}}^T\end{bmatrix}. \quad (62)$$

Hence $\mathrm{cov}_{\mathrm{con}}$ is obtained as

$$\mathrm{cov}_{\mathrm{con}} = \left(\mathbf{F}^T\mathbf{F}\right)^{-1}\mathbf{F}^T\mathrm{cov}_{\mathrm{un}}\,\mathbf{F}\left(\mathbf{F}^T\mathbf{F}\right)^{-1}. \quad (63)$$

Combining the property of Moore-Penrose inverse of matrix with above yields

$$\mathrm{cov}_{\mathrm{con}} = \left(\mathbf{F}^T\mathrm{cov}_{\mathrm{un}}^{-1}\,\mathbf{F}\right)^{-1}. \quad (64)$$

Substituting (40b) gives

$$\mathrm{cov}_{\mathrm{con}}^{-1} = \mathbf{F}^T\mathbf{G}_1^T\mathbf{Q}_n^{-1}\mathbf{G}_1\,\mathbf{F}. \quad (65)$$

Under small noise assumption, it can be verified through some algebraic manipulations that

$$\mathbf{F}^T\mathbf{G}_1^T\mathbf{B}_1^{-T} \approx \frac{\partial\mathbf{m}^{oT}}{\partial\mathbf{u}^o}. \quad (66)$$

Finally, substituting (48) in (65) and following the same procedures in Section IV-A, it can be shown that the GTRS in (55) can reach the CRLB

$$\mathrm{cov}_{\mathrm{con}} \approx \mathrm{CRLB}(\mathbf{u}^o). \quad (67)$$

C. MAXIMUM LIKELIHOOD ESTIMATION

The proposed two solutions (i.e., 2-step closed-form solution and GTRS solution) are designed to estimate the object location only. They cannot update the original parameters (nominal signal propagation speed c and sensor positions $\mathbf{p}$) to more accurate ones, which can be achieved theoretically in the analysis of CRLB. In this section, we will use the MLE to update c and $\mathbf{p}$.

A cost function is obtained from the logarithm likelihood function (10) by ignoring the constant items,

$$J(\boldsymbol{\alpha}^o) = (\boldsymbol{\gamma} - \boldsymbol{\gamma}^o(\boldsymbol{\alpha}^o))^T\mathbf{Q}_\gamma^{-1}(\boldsymbol{\gamma} - \boldsymbol{\gamma}^o(\boldsymbol{\alpha}^o)) \quad (68)$$

where $\boldsymbol{\gamma} = [\mathbf{m}^T, c, \mathbf{p}^T]^T$ and $\boldsymbol{\gamma}^o(\boldsymbol{\alpha}^o) = [\mathbf{m}^{oT}, c^o, \mathbf{p}^{oT}]^T$. $\boldsymbol{\gamma}^o(\boldsymbol{\alpha}^o)$ is a function of $\boldsymbol{\alpha}^o$. $\mathbf{Q}_\gamma^{-1}$ is

$$\mathbf{Q}_\gamma^{-1} = \begin{bmatrix}\mathbf{Q}_m^{-1} & & \\ & \sigma_c^{-2} & \\ & & \mathbf{Q}_p^{-1}\end{bmatrix}. \quad (69)$$

By using Taylor expansion, the nonlinear function $\boldsymbol{\gamma}^o(\boldsymbol{\alpha}^o)$ can be linearized as

$$\boldsymbol{\gamma}^o(\boldsymbol{\alpha}^o) \approx \boldsymbol{\gamma}^o(\boldsymbol{\alpha}_1) + \boldsymbol{\phi}_1(\boldsymbol{\alpha}^o - \boldsymbol{\alpha}_1), \tag{70}$$

where $\boldsymbol{\alpha}_1$ is an initial guess of $\boldsymbol{\alpha}^o$ and

$$\boldsymbol{\phi}_1 = \left.\frac{\partial \boldsymbol{\gamma}^o}{\partial \boldsymbol{\alpha}^T}\right|_{\boldsymbol{\alpha}=\boldsymbol{\alpha}_1}. \tag{71}$$

$\partial \boldsymbol{\gamma}^o / \partial \boldsymbol{\alpha}^T$ is in Appendix B. Substituting (70) in (68) and solving the equation $\partial J(\boldsymbol{\alpha}^o)/\partial \boldsymbol{\alpha}^o = \mathbf{0}_{2N+5}$ give

$$\boldsymbol{\alpha}^o = \boldsymbol{\alpha}_1 + \left(\boldsymbol{\phi}_1^T \mathbf{Q}_\gamma^{-1} \boldsymbol{\phi}_1\right)^{-1} \boldsymbol{\phi}_1^T \mathbf{Q}_\gamma^{-1} \left(\boldsymbol{\gamma} - \boldsymbol{\gamma}^o(\boldsymbol{\alpha}_1)\right). \tag{72}$$

This suggests an iterative algorithm, which iterates between $\boldsymbol{\alpha}^o$ and $\boldsymbol{\alpha}_1$. By replacing $\boldsymbol{\alpha}^o$ and $\boldsymbol{\alpha}_1$ with $\boldsymbol{\alpha}_{k+1}$ and $\boldsymbol{\alpha}_k$, we can obtain the following iterative equation

$$\boldsymbol{\alpha}_{k+1} = \boldsymbol{\alpha}_k + \left(\boldsymbol{\phi}_k^T \mathbf{Q}_\gamma^{-1} \boldsymbol{\phi}_k\right)^{-1} \boldsymbol{\phi}_k^T \mathbf{Q}_\gamma^{-1} \left(\boldsymbol{\gamma} - \boldsymbol{\gamma}^o(\boldsymbol{\alpha}_k)\right). \tag{73}$$

The reasonable initial guess for $\boldsymbol{\alpha}_k$ can be chosen as the nominal parameters (c, $\mathbf{t}$ and $\mathbf{s}_i$) combining with the object location obtained from the closed-form solution or GTRS solution.

When the proposed MLE method converges to the true location value (i.e., $\boldsymbol{\alpha}_{k+1} \approx \boldsymbol{\alpha}^o$), the theoretical covariance of this method shall be

$$\mathrm{cov}(\boldsymbol{\alpha}_{k+1}) \approx \left(\boldsymbol{\phi}^{oT} \mathbf{Q}_\gamma^{-1} \boldsymbol{\phi}^o\right)^{-1} \tag{74}$$

where $\boldsymbol{\phi}^o$ is the value by substituting $\boldsymbol{\alpha}^o$ in (71). Note that (74) has the same form as the the CRLB in (11). Substituting (71) and (82) in (74), after some straightforward algebraic derivation, we have

$$\left(\boldsymbol{\phi}^{oT} \mathbf{Q}_\gamma^{-1} \boldsymbol{\phi}^o\right)^{-1} = \mathrm{CRLB}(\boldsymbol{\alpha}^o). \tag{75}$$

Therefore, the proposed MLE solution can reach the CRLB.

However, extensive simulations show that the performance of the proposed MLE is sensitive to the sensor position noise. The iterative MLE will not converge due to some numerical problems when the sensor position noise becomes large. It is the intent of the simplified MLE that ignores the sensor position noise, and updates the propagation speed while reducing the complexity of the MLE. The simplified MLE in Remark 2 will maintain the estimation accuracy when the sensor position noise is small.

Remark 2: There are total $2N+5$ unknowns in the proposed MLE solution (73) and $2N+2$ unknowns come from the sensor positions. In reality, when the sensor position errors are not large, the CRLBs of them are near the nominal parameter RMSE. In addition, the analysis in Section III-B also shows that the performance increases in sensor position CRLBs are also limited. Therefore, the term $\ln f_3(\mathbf{p})$ in (10) can be ignored and a simplified recursive MLE solution to update c only is obtained as

$$\tilde{\boldsymbol{\alpha}}_{k+1} = \tilde{\boldsymbol{\alpha}}_k + \left(\tilde{\boldsymbol{\phi}}_k^T \tilde{\mathbf{Q}}_\gamma^{-1} \tilde{\boldsymbol{\phi}}_k\right)^{-1} \tilde{\boldsymbol{\phi}}_k^T \tilde{\mathbf{Q}}_\gamma^{-1} \left(\tilde{\boldsymbol{\gamma}} - \tilde{\boldsymbol{\gamma}}^o(\tilde{\boldsymbol{\alpha}}_k)\right), \tag{76}$$

where

$$\tilde{\boldsymbol{\gamma}} = [\mathbf{m}^T, c]^T \tag{77a}$$

$$\tilde{\boldsymbol{\alpha}}_k = [\mathbf{u}_k^T, c_k]^T \tag{77b}$$

$$\tilde{\boldsymbol{\gamma}}^o(\tilde{\boldsymbol{\alpha}}_k) = [\mathbf{m}^{oT}(\tilde{\boldsymbol{\alpha}_k}), c_k]^T \tag{77c}$$

$$\tilde{\boldsymbol{\phi}}_k = \partial \tilde{\boldsymbol{\gamma}}^o(\tilde{\boldsymbol{\alpha}}_k)/\partial \tilde{\boldsymbol{\alpha}_k}^T \tag{77d}$$

$$\tilde{\mathbf{Q}}_\gamma = \mathrm{diag}(\mathbf{Q}_m, \sigma_c^2). \tag{77e}$$

The complexity of MLE solution comes from the inverse of matrix. The size of the inverse matrix in (76) is 3, while it is $2N+5$ in (73). Hence, the complexity of (76) is much lower than that of (73).

V. SIMULATION

This section will examine the performance of the proposed solutions, i.e., the 2-step closed-form solution, the GTRS solution and the MLE solution. The former two solutions are used to obtain the position estimate and the MLE solution is used to update the nominal parameters which are also contaminated by Gaussian noise.

TABLE 1. Localization geometry: object positions $\mathbf{u}^o$, transmitter position $\mathbf{t}^o$ and receiver position $\mathbf{s}_i^o$.

(m)	$\mathbf{u}^o$	$\mathbf{t}^o$	$\mathbf{s}_1^o$	$\mathbf{s}_2^o$	$\mathbf{s}_3^o$	$\mathbf{s}_4^o$	$\mathbf{s}_5^o$
x	500	1500	-1000	2500	-3000	2000	-2000
y	2000	1500	3000	-500	1000	-4000	-2000

The localization geometry is based on [27] and it is shown in Table 1. The true acoustic transmission speed is $c^o = 1500$ m/s. The noise covariance matrix of time delay measurement is $\mathbf{Q}_\tau = (\sigma/c^o)^2\mathbf{I}$ and that of angle measurement is $\mathbf{Q}_\theta = \sigma_\theta^2 \mathbf{I}$. The covariance matrix for nominal sensor position is also set as a diagonal matrix $\mathbf{Q}_p = \sigma_p^2 \mathbf{I}$. The performance of the method will be evaluated in terms of root mean square error (RMSE) that is defined as

$$\mathrm{RMSE}(\mathbf{x}^o) = \sqrt{\frac{1}{K}\left(\sum_{k=1}^{K} \|\mathbf{x}_k - \mathbf{x}^o\|^2\right)}, \tag{78}$$

where K is the total number of trails and $\mathbf{x}_k$ is a estimate of the true value $\mathbf{x}^o$ for a given method in the ith trail. In the simulation, K is set to $K = 5000$. This section will present two sets of simulations. The first set presents the localization performance of the proposed methods and the second set investigates the parameter update using the proposed MLE method.

A. OBJECT POSITION ESTIMATION

We first investigate the performance of the proposed methods (denoted by "2 step" and "GTRS") when the measurement noise increases. The simplified 2-step closed-form solution (denoted by "Simplified 2 step") in Remark 1 and the the simulation based on the MLE in [36] assuming no parameter error are also included for comparison. The standard deviation of signal propagation speed is $\sigma_c = 5$ m/s and the sensor position noise is $\sigma_p = 1$ m.

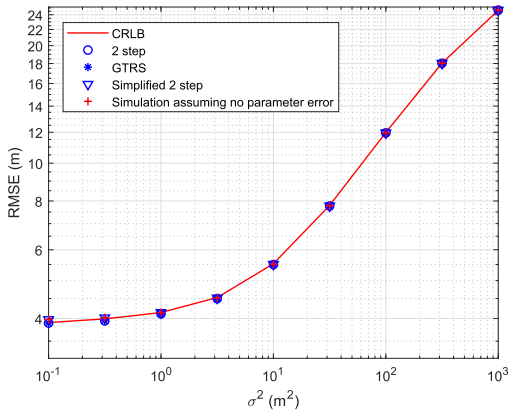

FIGURE 4. Localization performance when time measurement noise σ increases.

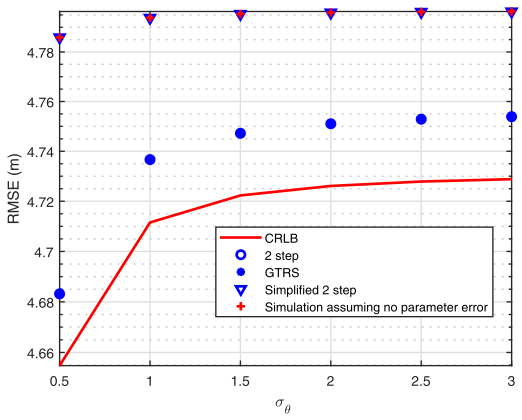

FIGURE 5. Localization performance when angle measurement noise σ_θ increases.

Fig. 4 shows the RMSE as the time measurement noise power increases when $\sigma_\theta = 1$ deg. The proposed methods work well and both of them can reach the CRLB. The simplified 2-step closed-form solution and the MLE solution when assuming no parameter error have the same performance. They both can also reach the CRLB when the time measurement noise is large, but the RMSEs will be gradually away from the CRLB when the measurement noise decreases. Fig. 5 illustrates the results in different level of the bearing angle measurement noise when $\sigma = 1$ m. The angle noise σ_θ has less effect on the localization performance because the value of CRLB in the figure is from 4.65 to 4.72. Although the RMSE of the proposed methods in this figure seems not to reach the CRLB, the steady gap is only about 0.02 and it is really a tiny value. The performance of the simplified 2-step solution will degrade at small angle noise. It has a wider gap (0.07 to 0.13) from the CRLB compared with the other 2 solutions.

In general, the proposed two methods have a good performance in different measurement noise level. Besides, the observations of the simplified 2-step method in Fig. 4 and Fig. 5 are consistent with the description in Remark 1 that the 2-step solution can be approximated by the simplified 2-step solution when the measurement noise (σ and/or σ_θ) is relatively large.

We next examine the RMSE when we fix the measurement noise. The time measurement noise is $\sigma = 1$ m and the angle measurement noise is $\sigma_\theta = 1$ deg.

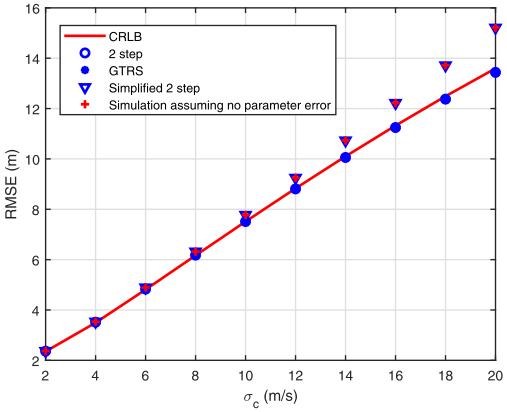

FIGURE 6. Localization performance when the noise of signal propagation speed increases.

Fig. 6 gives the results for the object position RMSE when the sensor position noise is fixed at $\sigma_p = 1$ m and the signal propagation speed noise σ_c varies from 2 m/s to 20 m/s. The proposed 2-step closed-form solution and the GTRS solution have the same performance and both of them can attain the CRLB. However, the simplified 2-step method is only accurate when σ_c is small. Its performance will deteriorate when large error appears in the signal propagation speed c. In Fig. 7, we fix $\sigma_c = 5$ m/s and vary σ_p from 0.5 m to 5 m. The observation is similar to Fig. 5 that the proposed two solutions have a small steady gap (about 0.02) from the CRLB. The simplified 2-step solution also has a gap, and the gap becomes wider when the sensor position error increases. Therefore, the proposed two solutions are more accurate than the simplified 2-step method.

B. NOMINAL PARAMETER UPDATE

This subsection will examine the proposed MLE solution (denoted by 'MLE') in (73) for updating the nominal parameters, i.e., signal propagation speed and sensor positions. The simplified MLE solution (denoted by 'Simplified MLE') in Remark 2 is also included for comparison, but it is used to update the signal propagation speed only. The time

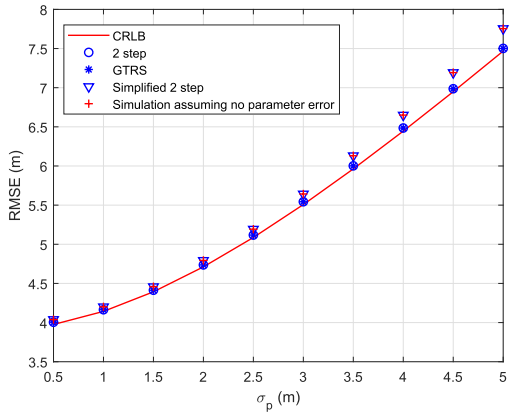

FIGURE 7. Localization performance when the noise of sensor position increases.

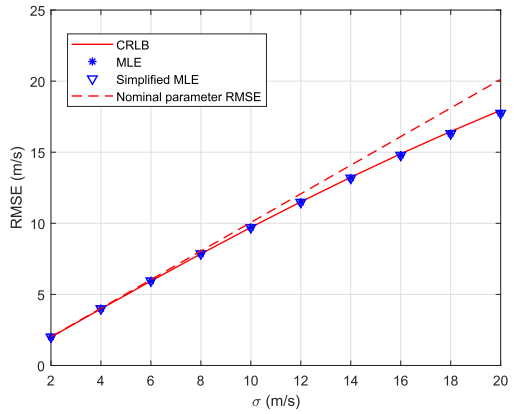

FIGURE 8. Update the signal propagation speed when the noise of signal propagation speed increases.

measurement noise is $\sigma = 1$ m and angle measurement noise is $\sigma_\theta = 1$ deg.

The RMSE of the signal propagation speed updated by MLE or simplified MLE is shown in Fig. 8. Both the two methods are able to reach the CRLB accuracy. The precision increase after updating the nominal signal propagation speed will be significant when σ_c is large. In other words, the nominal signal propagation speed can be updated to more accurate one when large error occurs in the signal propagation speed.

Fig. 9 shows the performance of the sensor positions updated by MLE. We have showed in Fig. 3 that the CRLBs for all sensor positions are lower than their nominal parameter RMSEs. However, the extensive Monte Carlo simulation tests show that not all sensor positions are able to converge to the same accuracy as defined by the CRLB using the proposed MLE. In this simulation, although the RMSE of the sensor position $\mathbf{s}_2$ can reach the CRLB, the accuracy increase in position is negligible. The average CRLB (or average MLE) in Fig. 9 represents the average value of all sensor position CRLBs (or sensor position RMSEs of MLE). For most sensors, the proposed MLE can not reach the CRLB when updating the sensor positions. One reason is that the high order terms in (70) related to unknowns are ignored and this approximation is not enough for updating the sensor

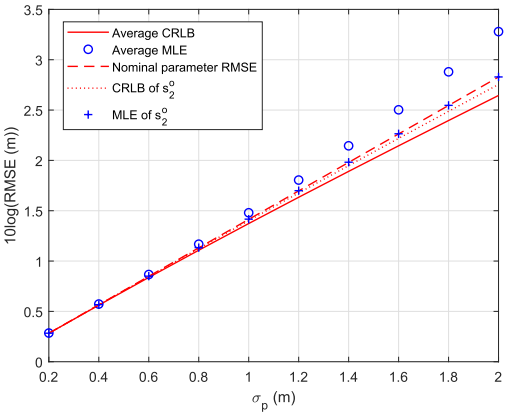

FIGURE 9. Update the sensor positions when the noise of sensor position increases.

positions accurately. The other reason is that the chance of having numerical problem will be high with $2N+5$ unknowns especially when the sensor position noise increases.

VI. CONCLUSION

This paper investigated the problem of multistatic sonar localization with a transmitter where the signal transmission speed, the transmitter and receiver positions are all contaminated by Gaussian noise. Two solutions were proposed to estimate the object position using the time measurements and angle measurements as well as the distribution of the nominal parameters. One is a 2-step closed-form solution using weighted least squares and the other is the GTRS solution using Newton's method. Both methods are simple and can reach the CRLB. In addition, analysis of the CRLB demonstrated that the nominal parameters which are used for localization can also be updated to more accurate ones. Therefore, a MLE solution was derived to update the nominal parameters. Simulations show that the precision increase in signal propagation speed is significant when the propagation speed noise is large.

ACKNOWLEDGMENT

The authors would like to thank the Editor and the anonymous reviewers for their valuable comments and suggestions.

APPENDIX A

$$\frac{\partial \mathbf{m}^o}{\partial \boldsymbol{\alpha}^{oT}} = \begin{bmatrix} \partial \boldsymbol{\tau}^o/\partial \mathbf{u}^{oT} & \partial \boldsymbol{\tau}^o/\partial c^o & \partial \boldsymbol{\tau}^o/\partial \mathbf{p}^{oT} \\ \partial \boldsymbol{\theta}^o/\partial \mathbf{u}^{oT} & \mathbf{O} & \partial \boldsymbol{\theta}^o/\partial \mathbf{p}^{oT} \end{bmatrix} \tag{79}$$

The elements in (79) are expressed as

$$\partial \boldsymbol{\tau}^o/\partial \mathbf{u}^{oT} = \left[\partial \tau_1^o/\partial \mathbf{u}^o, \cdots, \partial \tau_N^o/\partial \mathbf{u}^o\right]^T, \tag{80a}$$

$$\partial \boldsymbol{\tau}^o/\partial c = \left[\partial \tau_1^o/\partial c, \cdots, \partial \tau_N^o/\partial c\right]^T, \tag{80b}$$

$$\partial \boldsymbol{\tau}^o/\partial \mathbf{p}^{oT} = \left[\partial \tau_1^o/\partial \mathbf{p}^o, \cdots, \partial \tau_N^o/\partial \mathbf{p}^o\right]^T, \tag{80c}$$

$$\partial \boldsymbol{\theta}^o/\partial \mathbf{u}^{oT} = \left[\partial \theta_1^o/\partial \mathbf{u}^o, \cdots, \partial \theta_N^o/\partial \mathbf{u}^o\right]^T, \tag{80d}$$

$$\partial \boldsymbol{\theta}^o/\partial \mathbf{p}^{oT} = \left[\partial \theta_1^o/\partial \mathbf{p}^o, \cdots, \partial \theta_N^o/\partial \mathbf{p}^o\right]^T, \tag{80e}$$

where

$$\partial\tau_i^o/\partial\mathbf{u}^o = (\boldsymbol{\rho}_{\mathbf{u}^o-\mathbf{t}} + \boldsymbol{\rho}_{\mathbf{u}^o-\mathbf{s}_i})/c, \tag{81a}$$

$$\partial\tau_i^o/\partial c = -\tau_i^o/c, \tag{81b}$$

$$\partial\tau_i^o/\partial\mathbf{p}^o = \left[\partial\tau_i^o/\partial\mathbf{t}^{oT}, \partial\tau_i^o/\partial\mathbf{s}_1^{oT}, \cdots, \partial\tau_i^o/\partial\mathbf{s}_N^{oT}\right]^T, \tag{81c}$$

$$\partial\tau_i^o/\partial\mathbf{t}^{oT} = -(\boldsymbol{\rho}^T_{\mathbf{u}^o-\mathbf{t}} + \boldsymbol{\rho}^T_{\mathbf{t}-\mathbf{s}_i})/c, \tag{81d}$$

$$\partial\tau_i^o/\partial\mathbf{s}_i^{oT} = (-\boldsymbol{\rho}^T_{\mathbf{u}^o-\mathbf{s}_i} + \boldsymbol{\rho}^T_{\mathbf{t}-\mathbf{s}_i})/c, \tag{81e}$$

$$\partial\theta_i^o/\partial\mathbf{u}^o = [s_{i,y}^o - y^o, x^o - s_{i,x}^o]^T/\|\mathbf{u}^o - \mathbf{s}_i^o\|^2, \tag{81f}$$

$$\partial\theta_i^o/\partial\mathbf{p}^o = \left[0, 0, \partial\theta_i^o/\partial\mathbf{s}_1^{oT}, \cdots, \partial\theta_i^o/\partial\mathbf{s}_N^{oT}\right]^T, \tag{81g}$$

$$\partial\theta_i^o/\partial\mathbf{s}_i^{oT} = [y^o - s_{i,y}^o, s_{i,x}^o - x^o]/\|\mathbf{u}^o - \mathbf{s}_i^o\|^2, \tag{81h}$$

Note that $\partial\tau_i^o/\partial\mathbf{s}_j^{oT}$ and $\partial\theta_i^o/\partial\mathbf{s}_j^{oT}$ $(i \neq j)$ are zero vectors.

APPENDIX B

$$\frac{\partial\boldsymbol{\gamma}^o}{\partial\boldsymbol{\alpha}^T} = \begin{bmatrix} \partial\boldsymbol{\gamma}^o/\partial\mathbf{u}^T & \partial\boldsymbol{\gamma}^o/\partial c & \partial\boldsymbol{\gamma}^o/\partial\mathbf{p}^T \\ \mathbf{0}_2^T & 1 & \mathbf{0}_{2N+2}^T \\ \mathbf{O} & \mathbf{O} & \mathbf{I} \end{bmatrix} \tag{82}$$

where $\partial\boldsymbol{\gamma}^o/\partial\mathbf{u}^T$, $\partial\boldsymbol{\gamma}^o/\partial c$ and $\partial\boldsymbol{\gamma}^o/\partial\mathbf{p}^T$ have the same expressions in Appendix A by replacing the true value $\boldsymbol{\alpha}^o$ with $\boldsymbol{\alpha}$.

REFERENCES

[1] Y. Sun and Q. Wan, "Position determination for moving transmitter using single station," *IEEE Access*, vol. 6, pp. 61103–61116, Oct. 2018.
[2] T. Jia, H. Wang, X. Shen, X. Liu, and H. Jing, "Bearing-only multiple sources localization and the spatial spectrum," in *Proc. IEEE Oceans*, Aberdeen, Scotland, Jun. 2017, pp. 1–5.
[3] X. Chen, D. Wang, J. Yin, and Y. Wu, "Performance analysis and dimension-reduction Taylor series algorithms for locating multiple disjoint sources based on TDOA under synchronization clock bias," *IEEE Access*, vol. 6, pp. 48489–48509, Aug. 2018.
[4] B. Oudompheng, B. Nicolas, and L. Lamotte, "Localization and contribution of underwater acoustical sources of a moving surface ship," *IEEE J. Ocean. Eng.*, vol. 43, no. 2, pp. 536–546, Apr. 2018.
[5] I. Bergel and Y. Noam, "Lower bound on the localization error in infinite networks with random sensor locations," *IEEE Trans. Signal Process.*, vol. 66, no. 5, pp. 1228–1241, Mar. 2018.
[6] G. Jingjie, S. Xiaohong, M. Haodi, J. Tianyi, W. Ling, and W. Haiyan, "A range-angle based self-localization scheme for MUANS," in *Proc. OCEANS-Aberdeen*, Jun. 2017, pp. 1–4.
[7] Y. Sun, K. C. Ho, and Q. Wan, "Solution and analysis of TDOA localization of a near or distant source in closed form," *IEEE Trans. Signal Process.*, vol. 67, no. 2, pp. 320–335, Jan. 2019.
[8] T. Jia, H. Wang, X. Shen, J. Gao, and X. Liu, "An accurate TDOA-AOA localization method using structured total least squares," in *Proc. IEEE Oceans*, Aberdeen, Jun. 2017, pp. 1–5.
[9] G. Wang, Y. Li, N. Ansari, "A semidefinite relaxation method for source localization using TDOA and FDOA measurements," *IEEE Trans. Veh. Technol.*, vol. 62, no. 2, pp. 853–862, Feb. 2013.
[10] Y. Yan, X. Shen, F. Hua, and X. Zhong, "On the semidefinite programming algorithm for energy-based acoustic source localization in sensor networks," *IEEE Sensors J.*, vol. 18, no. 21, pp. 8835–8846, Nov. 2018.
[11] K. C. Ho, "Bias reduction for an explicit solution of source localization using TDOA," *IEEE Trans. Signal Process.*, vol. 60, no. 5, pp. 2101–2114, May 2012.
[12] T. Jia, H. Wang, X. Shen, Z. Jiang, and K. He, "Target localization based on structured total least squares with hybrid TDOA-AOA measurements," *Signal Process.*, vol. 143, pp. 211–221, Feb. 2018.
[13] A. Noroozi and M. A. Sebt, "Algebraic solution for three-dimensional TDOA/AOA localisation in multiple-input–multiple-output passive radar," *IET Radar, Sonar Navigation*, vol. 12, no. 1, pp. 21–29, 2017.
[14] S. Simakov, "Localization in Airborne Multistatic Sonars," *IEEE J. Ocean. Eng.*, vol. 33, no. 3, pp. 278–288, Jul. 2008.
[15] S. Coraluppi, "Multistatic sonar localization," *IEEE J. Ocean. Eng.*, vol. 31, no. 4, pp. 964–974, Oct. 2006.
[16] Y.-T. Chan, H. Y. C. Hang, and P.-C. Ching, "Exact and approximate maximum likelihood localization algorithms," *IEEE Trans. Veh. Technol.*, vol. 55, no. 1, pp. 10–16, Jan. 2006.
[17] Y. Wang and K. C. Ho, "TDOA positioning irrespective of source range," *IEEE Trans. Signal Process.*, vol. 65, no. 6, pp. 1447–1460, Mar. 2017.
[18] Y. T. Chan and K. C. Ho, "A simple and efficient estimator for hyperbolic location," *IEEE Trans. Signal Process.*, vol. 42, no. 8, pp. 1905–1915, Aug. 1994.
[19] K. C. Ho and W. Xu, "An accurate algebraic solution for moving source location using TDOA and FDOA measurements," *IEEE Trans. Signal Process.*, vol. 52, no. 9, pp. 2453–2463, Sep. 2004.
[20] L. Yang, L. Yang, and K. C. Ho, "Moving target localization in multistatic sonar by differential delays and Doppler shifts," *IEEE Signal Process. Lett.*, vol. 23, no. 9, pp. 1160–1164, Sep. 2016.
[21] A. Beck, P. Stoica, and J. Li, "Exact and approximate solutions of source localization problems," *IEEE Trans. Signal Process.*, vol. 56, no. 5, pp. 1770–1778, May 2008.
[22] J. Zheng, K. W. Lui, and H.-C. So, "Accurate three-step algorithm for joint source position and propagation speed estimation," *Signal Process.*, vol. 87, no. 12, pp. 3096–3100, Dec. 2007.
[23] R. Rabenstein and P. Annibale, "Acoustic source localization under variable speed of sound conditions," *Wireless Commun. Mobile Comput.*, vol. 2017, Oct. 2017, Art. no. 9524943.
[24] R. Diamant and L. Lampe, "Underwater localization with time-synchronization and propagation speed uncertainties," *IEEE Trans. Mobile Comput.*, vol. 12, no. 7, pp. 1257–1269, Jul. 2013.
[25] L. Yang, L. Yang, and K. C. Ho, "Moving target localization in multistatic sonar using time delays, Doppler shifts and arrival angles," in *Proc. IEEE Int. Conf. Acoust., Speech, Signal Process.*, Mar. 2017, pp. 3399–3403.
[26] K. C. Ho, X. Lu, and L. Kovavisaruch, "Source localization using TDOA and FDOA measurements in the presence of receiver location errors: Analysis and solution," *IEEE Trans. Signal Process.*, vol. 55, no. 2, pp. 684–696, Feb. 2007.
[27] L. Rui and K. C. Ho, "Efficient closed-form estimators for multistatic sonar localization," *IEEE Trans. Aerosp. Electron. Syst.*, vol. 51, no. 1, pp. 600–614, Jan. 2015.
[28] K. V. MacKenzie, "Nine-term equation for sound speed in the oceans," *Acoust. Soc. Amer. J.*, vol. 70, pp. 807–812, Sep. 1981.
[29] C. T. Chen and F. J. Millero, "Speed of sound in seawater at high pressures," *J. Acous. Soc. Amer.*, vol. 62, no. 5, pp. 1129–1135, Nov. 1977.
[30] B. Zhang, Y. Hu, H. Wang, and Z. Zhuang, "Underwater source localization using TDOA and FDOA measurements with unknown propagation speed and sensor parameter errors," *IEEE Access*, vol. 6, p. 36 645–36 661, Jul. 2018.
[31] A. Mahajan and M. Walworth, "3D position sensing using the differences in the time-of-flights from a wave source to various receivers," *IEEE Trans. Robot. Autom.*, vol. 17, no. 1, pp. 91–94, Feb. 2001.
[32] C. He, Y. Wang, C. Chen, and X. Guan, "Target localization for a distributed SIMO ssonar with an isogradient sound speed profile," *IEEE Access*, vol. 6, pp. 29770–29783, Jun. 2018.
[33] X. Guo, K. Yang, Q. Yang, S. Zhu, R. Cao, and Y. Ma, "Tracking-positioning of sound speed profiles and moving acoustic source in shallow water," in *Proc. IEEE Oceans*, Kobe, Japan, Oct. 2016, pp. 366–369.
[34] R. Játiva and J. Vidal, "Cramer-Rao bounds in the estimation of time of arrival in fading channels," *EURASIP J. Adv. Signal Process.*, vol. 2018, no. 1, p. 19, Mar. 2018.
[35] T. Jia, H. Wang, X. Shen, and X. Liu, "Direction of arrival estimation with co-prime arrays via compressed sensing methods," in *Proc. OCEANS-Shanghai*, Shanghai, China, Apr. 2016, pp. 1–5.
[36] S. M. Kay, *Fundamentals of Statistical Signal Processing: Estimation Theory*, vol. 1. Upper Saddle River, NJ, USA: Prentice-Hall, 1993.
[37] J. J. Moré, "Generalizations of the trust region problem," *Optim. Methods Softw.*, vol. 2, nos. 3–4, pp. 189–209, Jan. 1993.

TIANYI JIA received the B.S. degree in information and computing science from Northwestern Polytechnical University, Xi'an, China, in 2014, where he is currently pursuing the Ph.D. degree with the Department of Electronics and Communication Engineering, and is a Visiting Student of the Department of Electrical and Computer Engineering, University of Missouri, Columbia, USA. His current research interests include source localization and sensor array processing.

XIAOHONG SHEN received the B.S., M.S., and Ph.D. degrees in electrical engineering from Northwestern Polytechnical University (NPU), Xi'an, China, in 1987, 1998, and 2008, respectively, where she is currently a Full Professor with the School of Marine Science and Technology. Her research interests include signal processing and underwater acoustic communication and networking. Recently, her research focuses are on underwater acoustic high data rate communication and underwater acoustic sensor networks.

HAIYAN WANG received the B.S., M.S., and Ph.D. degrees from the School of Marine Science and Technology, Northwestern Polytechnical University (NPU), Xi'an, China, in 1987, 1990, and 2004, respectively, all in electrical engineering. He has been a Faculty Member of NPU, since 1990, and a Professor, since 2004. He teaches and conducts research at NPU in the areas of signal and information processing, electronic engineering, and tracking and locating of maneuvering targets. His general research interests include modern signal processing, array signal processing, underwater acoustic communications, tracking and locating of maneuvering targets, and data mining technique and its application.